Appl Phys A (2012) 107:127–132
DOI 10.1007/s00339-011-6753-x

Applied Physics A
Materials Science & Processing

INVITED PAPER

Waveguiding effect in 2D metal–dielectric–metal grating structure

Eunice S.P. Leong · Y.J. Liu · C.C. Chum · B. Wang · J.H. Teng

Received: 11 July 2011 / Accepted: 8 December 2011 / Published online: 28 December 2011

Abstract We have studied the waveguiding effect in a 2D metal–dielectric–metal (MDM) grating structure formed on a quartz substrate. The grating was first formed via e-beam lithography and subsequently covered by Ag/MgF_2/Ag MDM films. At a pitch of 300 nm in both x- and y-directions, low reflectance and transmittance were observed in the UV–VIS range, indicating efficient coupling of normal incident light into waveguiding modes. As evidence, we measured the spectrum of the waveguide from the edge, and the bandwidth of the spectrum was as narrow as ∼74 nm. The bandwidth of the waveguide can be further improved by increasing the MDM stack number. In addition, the bandwidth can also be widened by increasing the pitch of the structure. The physical mechanism underlying the phenomena was analyzed and experimentally confirmed. Such effect could be useful in many applications, such as DFB lasers, solar cells, waveguides, and light emitting devices.

1 Introduction

Gratings are a crucial optical component in spectroscopy for a wide range of applications including physical, astronomical, biological, chemical, metallurgical, and other analytical investigations. In quantum mechanics, grating spectrometers are firstly used to verify predictions regarding the spectrum of hydrogen. In astrophysics, gratings provide clues to the composition of and processes in stars and planetary atmospheres, as well as the large-scale motions of objects in the universe. In chemistry and biology, grating-based sensors are used to detect the presence and concentration of chemical/biological species in samples.

Recently, gratings have received intense attention in plasmonics because they can be used to efficiently couple free-space light to surface plasmons by bridging the momentum gap between them [1–3]. Conversely, surface plasmons can also enhance the grating diffraction [4–9]. Interactions at the interface between a grating and metal nanostructure are usually complicated. On the other hand, in a grating incorporated with gain materials, the grating can provide a distributed feedback (DFB) of the optical signals without the need of two discrete mirrors to form the cavity, thus amplifying the signals—the working principle for DFB lasers [10]. An efficient conversion process between photons and plasmons could greatly decrease the laser threshold and increase the quality factor. Previously, we have investigated the optical properties of the metal–dielectric–metal (MDM) thin film systems and found that an efficient photon–plasmon–photon conversion process could be achieved by controlling the surface roughness of the top silver surface [11].

In this paper, we shall study the waveguiding effect in a two-dimensional (2D) MDM-coated dielectric grating structure on a quartz substrate. The transmittance and reflectance of the MDM-coated dielectric grating were measured using a UV–VIS–NIR optical spectrometer. The waveguided edge emission of the grating was also measured using an Ocean-Optics USB spectrometer. The edge emission was compared between pure dielectric and MDM-coated dielectric gratings. We found that the MDM-coated dielectric grating provides a spectrum with higher peak intensity as well as much narrower bandwidth compared to the uncoated one. The underlying mechanism was discussed based on the simulation. This study could be useful in many applications, such as enhancement of absorption in solar cells, improvement of cou-

E.S.P. Leong · Y.J. Liu · C.C. Chum · B. Wang · J.H. Teng (✉)
Institute of Materials Research and Engineering, Agency for Science Technology and Research (A*STAR), 3 Research Link, Singapore 117602, Singapore
e-mail: jh-teng@imre.a-star.edu.sg

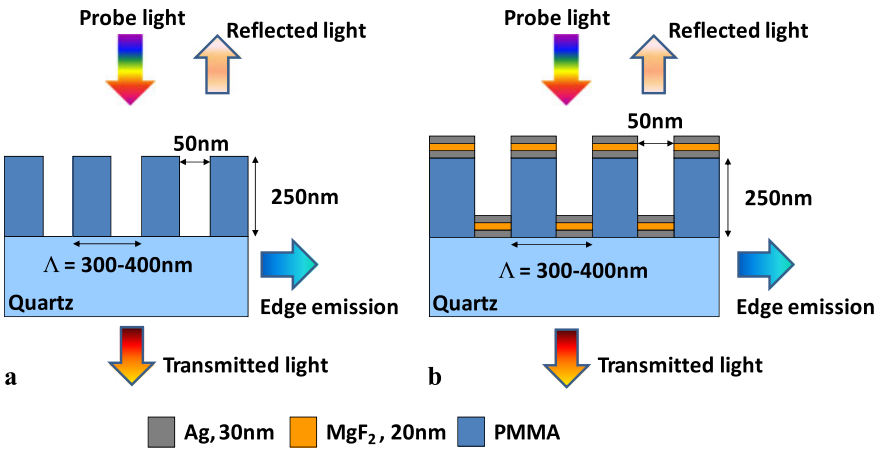

Fig. 1 Schematic of (**a**) PMMA grating and (**b**) PMMA grating with MDM film overlayer. The spectra measurement is also schematically shown in both (**a**) and (**b**)

pling in waveguides, and enhancement of light emission in light emitting devices.

2 Experimental

2.1 Sample fabrication

A 15 mm × 15 mm × 0.4 mm quartz substrate with refractive index 1.46 was first cleaned with acetone and isopropyl alcohol (IPA) in an ultrasonic bath. To fabricate the PMMA grating structure via e-beam lithography technique, PMMA 950k with refractive index ∼1.49 was spin coated on the bare quartz to form a thickness of 250–300 nm. Pre-baking was carried out at 170°C for 15 min. We then spin-coated a thin layer of e-spacer and baked the sample at 95°C for 2 min. E-beam lithography was carried out with ELIONIX ELS-7000. The current and voltage used were 50 pA and 100 kV, respectively. The fabricated patterns consist of gratings with the gap of 50 nm and the pitch fixed at 300 nm in the x-direction and pitches varying from 300 to 400 nm with 50 nm increments in the y-direction. Each pattern area is 150 × 150 μm^2. After e-beam writing, the e-spacer was removed with water. Pattern development was done in MIBK:IPA (1:3) for 70 seconds. Before evaporation, a short descum was carried out to remove any residual resist on the substrate using RIE Etcher (Plasmalab 80plus, Oxford) at 60 mtorr chamber pressure, 60 W electric power, 60 sccm oxygen flow rate for 5 seconds. Ag (30 nm)/MgF_2 (20 nm)/Ag (30 nm) films were thermally evaporated in an Auto306 (Edwards) thermal evaporator. The deposition rate for each layer was controlled to 1.4 ± 0.2 nm/min. Figure 1 shows the schematic of (a) PMMA grating and (b) PMMA grating with MDM overlayer.

2.2 Spectra measurement

Optical reflectance and transmission spectra were measured with an unpolarized probe light beam using a UV–VIS–NIR microspectrophotometer (CRAIC QDI 2010™), as shown in Fig. 1(b). The probe light beam was focused to have a detecting area of 7.1 × 7.1 μm^2 using a 36× objective lens combined with a variable aperture. An Ocean-Optics USB spectrometer with a fiber connection was used to measure the light observed from the edge of the quartz.

3 Results and discussion

Figures 2(a) and 2(b) show the SEM images of a PMMA grating and a MDM-coated PMMA grating. The grating period is $\Lambda_x = \Lambda_y = 300$ nm. After the deposition of MDM layers, the surface becomes rough due to Volmer–Weber growth mode of Ag [11]. It is also clear that the gap distance become smaller after the deposition.

Figure 3(a) shows the measured transmittance and reflectance spectra of the PMMA grating, while Fig. 3(b) shows the emission spectrum from the edge of the PMMA grating. Since the refractive index of PMMA layer is larger than that of quartz substrate, a certain amount of the photons is coupled into the waveguide inside the PMMA grating layer. As a result, the normally incident light was coupled into in-plane waveguide. Therefore, we observed a colored emission, as shown in the inset of Fig. 3(b). From Figs. 3(a) and 3(b), the edge emission spectrum approximately corresponds to the reflection dip from ∼400 to ∼600 nm. Upon deposition of MDM layers, both the reflectance and transmission spectra have been modified, as shown in Fig. 4(a). There is a broad reflection spectrum with a peak at ∼600 nm and a broad transmission due to the absorption of MDM structures. More importantly, we observed a significant enhancement of the edge emission for the MDM-coated PMMA grating: a much narrower emission spectrum with stronger peak intensity, as shown in Fig. 4(b). The inset of Fig. 4(b) shows a much clearer color purity compared to the pure PMMA grating case (see the inset of Fig. 3(b)). Therefore, the MDM-coated grating can

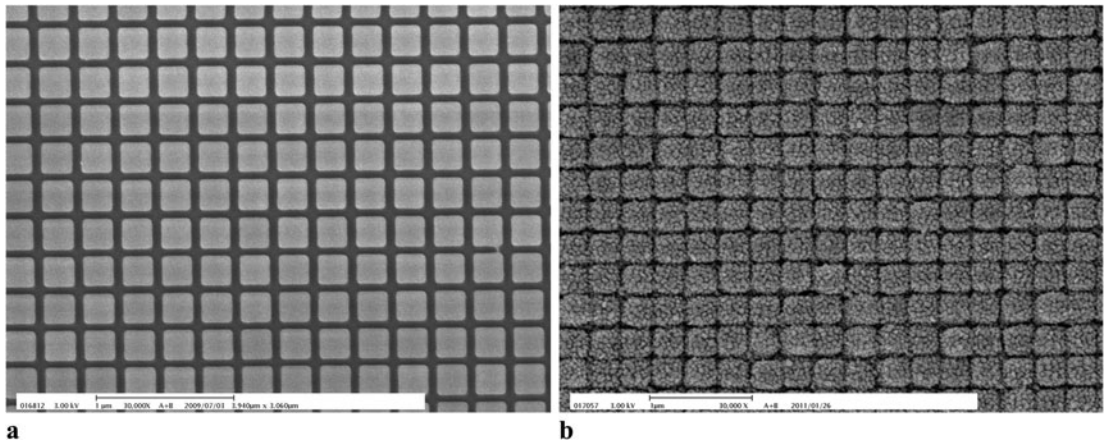

Fig. 2 SEM images of PMMA grating with $\Lambda_x = \Lambda_y = 300$ nm (**a**) before and (**b**) after MDM deposition

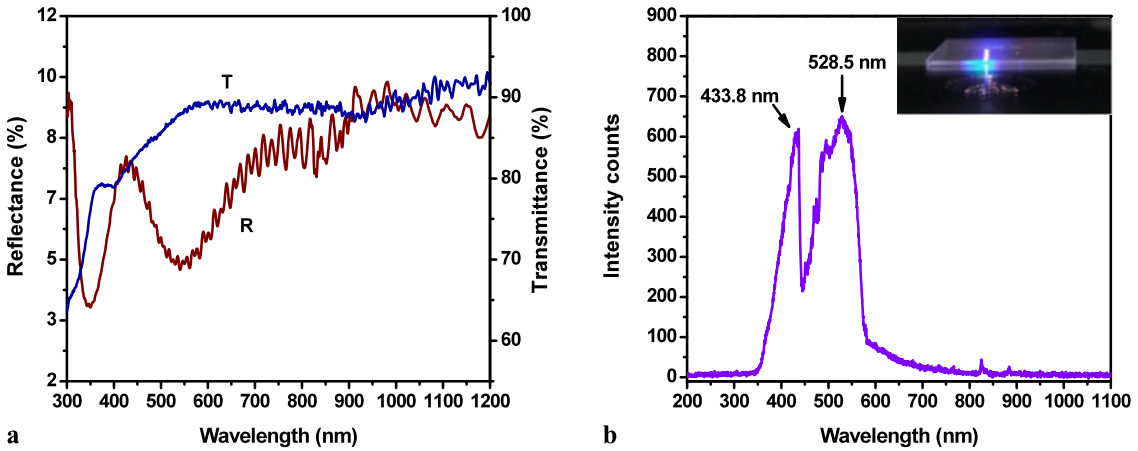

Fig. 3 Reflectance and transmittance (**a**) and edge emission (**b**) spectra of the PMMA grating. *Inset* shows the image of the light captured from the edge of the quartz substrate

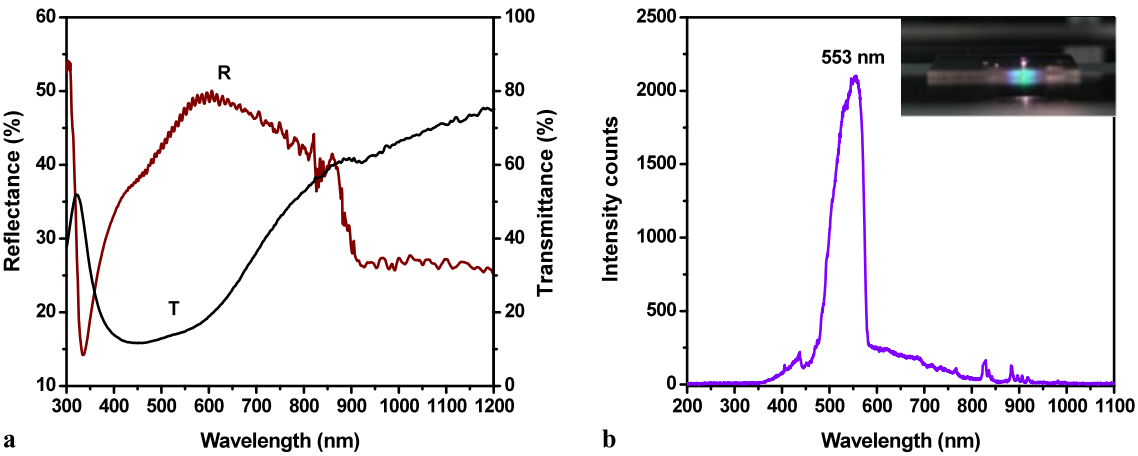

Fig. 4 Reflectance and transmittance (**a**) and edge emission (**b**) spectra of 1 stack of MDM-coated grating. *Inset* shows the image of the light captured from the edge of the quartz substrate

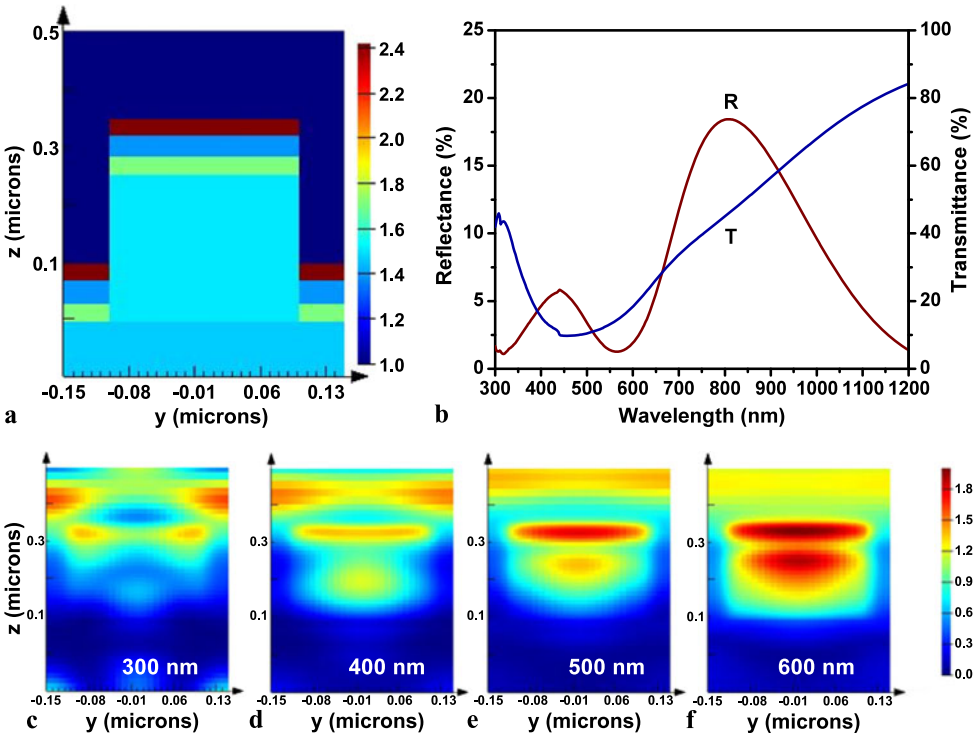

Fig. 5 (**a**) The simulation unit of the MDM-coated grating, (**b**) simulated reflectance and transmittance, (**c**)–(**f**) the field intensity distribution inside the gap for different light wavelengths with the same intensity scale

greatly improve the coupling from the out-of-plane incident light to the in-plane propagation light. We believe that the excited surface plasmons contribute greatly to this enhancement.

The simulation on the MDM-coated grating was carried out to confirm our prediction using the finite-difference time-domain (FDTD, Lumerical) method. Figure 5(a) shows the simulation unit of the MDM-coated grating. The simulation results are shown in Figs. 5(b)–5(f). Comparing the experimental (Fig. 4(a)) and simulation results (Fig. 5(b)), the transmission shows similar curves, while the reflection shows obvious offset in the reflection peaks and dips. The offset could arise from the difference between the ideal model and the real sample. In the model, the surface roughness and the gap reduction are ignored. Figures 5(c)–5(f) show the field intensity distribution for different light wavelengths in the visible range. From Figs. 5(c)–5(f), it can be seen that most of the light localized on the top with the same height of top MDM layer, which is due to excitation of surface plasmons, while more light start to leak into the PMMA grating layer after 500 nm wavelength. In our experiment, since the PMMA grating period is much less than the visible light wavelength, the diffraction of the grating is strongly suppressed. However, the top periodic Ag surface can effectively alter the wave vector of the light such that light of higher wave vector can be coupled into surface plasmons at the air/Ag interface. Since the gap is only 50 nm, the excited surface plasmons can couple to each other. Therefore, most of the light localizes at the top MDM layer. In addition, the surface plasmon momentum can match the momentum of the incident photon and the grating [12, 13], thus enhancing the light coupling due to the surface plasmon resonances associated with the localized waveguide resonance [14]. At the bottom layer of the MDM structure, the resonant surface plasmons can re-radiate into photons when the momentum gap between plasmons and photons is bridged by the grating. The re-radiated photons again will propagate laterally in the waveguide formed inside the PMMA layer. As a result, we observed a much narrower and stronger edge emission spectrum. Therefore, the MDM grating can greatly enhance the photon–plasmon–photon conversion efficiency. To further confirm this hypothesis, we deposited three stacks of such kind of MDM structures on the PMMA grating and measured the edge emission again.

Figure 6 shows the measured the spectrum and the CCD captured image (the inset). A much narrower spectrum was achieved compared to the single stack of MDM structures, which indicates that the more the number of stacks is, the narrower the edge emission. However, there exists a trade-off between the loss induced by the metals and the number of the MDM stacks. It can be seen from Fig. 6 that the intensity is slightly lower than the single stack case but still much higher than the pure PMMA grating. It is expected that with the increase of the stack numbers, the emission spectrum will have an even narrow bandwidth but greatly decreased intensity.

As a further step, the coupling effect of MDM structures is investigated by varying the grating period. In this case,

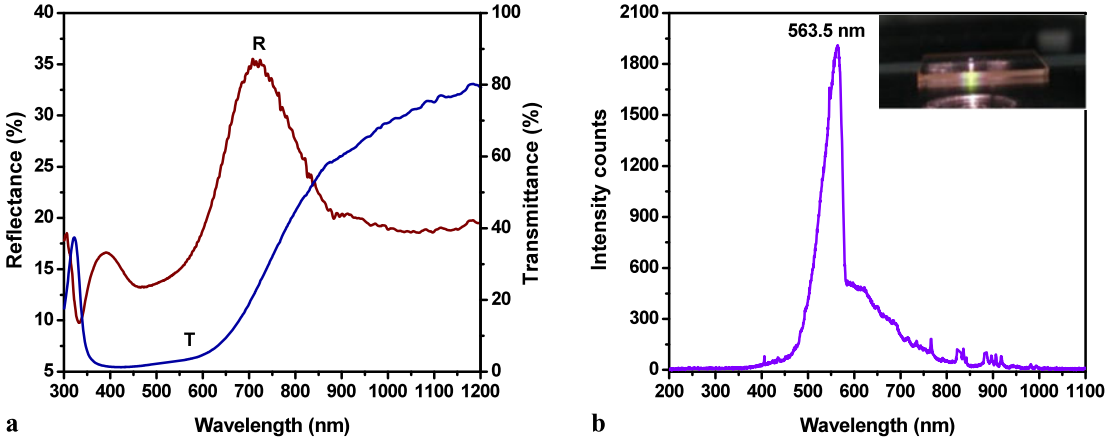

Fig. 6 Reflectance and transmittance (**a**) and edge emission (**b**) of 3 stacks of MDM-coated grating. *Inset* shows the image of the light that travels to the edge of the quartz

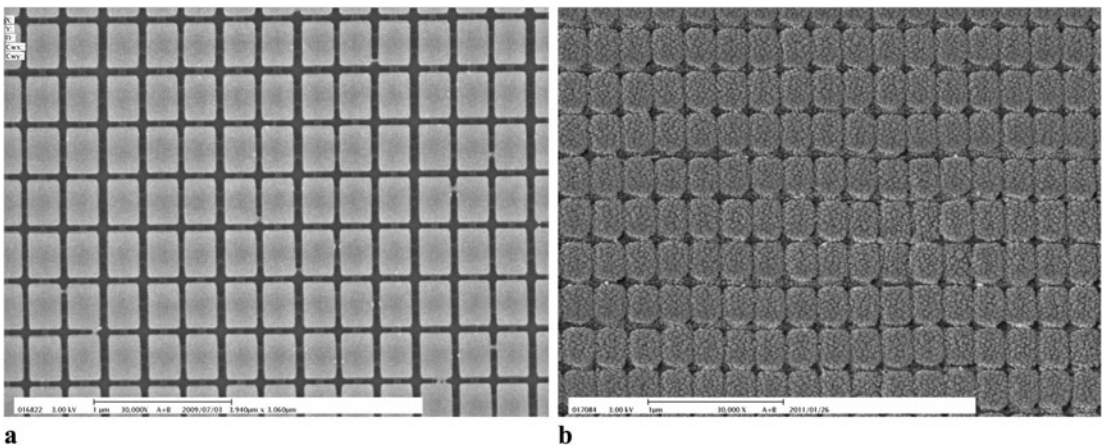

Fig. 7 SEM images of PMMA grating with $\Lambda_x = 300$ nm and $\Lambda_y = 400$ nm (**a**) before and (**b**) after MDM deposition

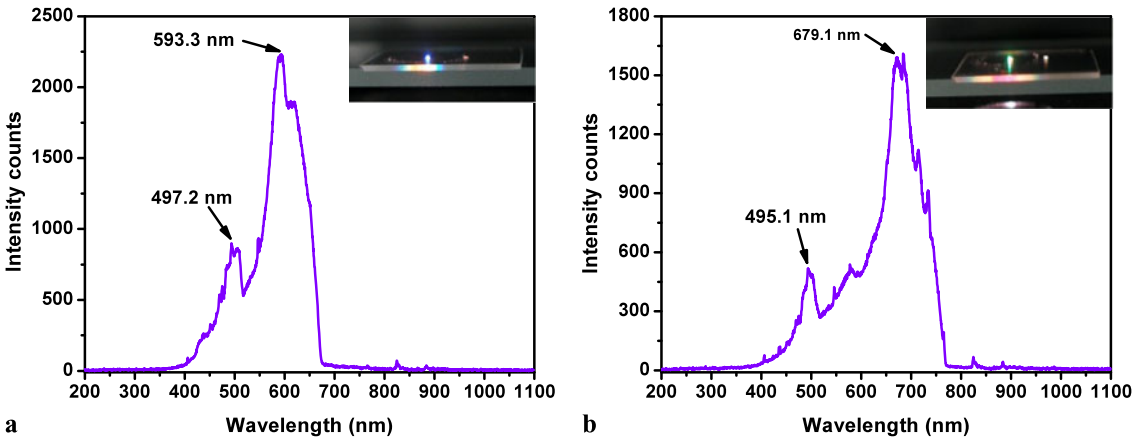

Fig. 8 Edge emission and image of light travelling to edge of the quartz measured in the y-direction for $\Lambda_y = 350$ nm (**a**) and $\Lambda_y = 400$ nm (**b**)

the grating period was fixed along the x-direction, $\Lambda_x = 300$ nm, but increased to $\Lambda_y = 350$ nm and $\Lambda_y = 400$ nm along the y-direction, respectively. Figures 7(a) and 7(b) show the SEM images of a PMMA grating and a MDM-coated PMMA grating. A clear difference in periodicity was observed along the x-direction and the y-direction. Very similar surface morphology can be also observed before and after the deposition of the MDM structures. We measured the edge emission spectra from both the x-direction and the y-direction. The emission along the x-direction was very similar to the case of $\Lambda_x = \Lambda_y = 300$ nm. However, the y-direction emission was very different. Figure 8 shows the measured y-direction emission spectra for $\Lambda_y = 350$ nm and $\Lambda_y = 400$ nm and their corresponding emission colors captured by the CCD. We can see that the bandwidth of emission becomes broader and the emission peaks red-shifted as the grating period increases.

4 Conclusions

We have studied the waveguiding effect in a 2D metal–dielectric–metal (MDM) grating structure formed on a quartz substrate. Such a MDM-coated PMMA gratings can efficiently couple the normally (vertically) incident light into the in-plane waveguided light. The MDM greatly enhanced the waveguide emission intensity due to the efficient photon–plasmon–photon conversion process. With the increase of the MDM stack numbers, the waveguide emission spectrum became narrower in bandwidth but lower in intensity. By increasing the pitch of the PMMA grating, the bandwidth was widened and the emission peak had a red-shift. The structure could be potentially useful in many applications, such as DFB lasers, solar cells, waveguides, and light emitting devices.

Acknowledgements This work was financially supported by Agency for Science, Technology and Research (A*STAR), under the grants Nos. 0921540099, 0921540098 and 0921450030.

References

1. H. Raether, *Surface Plasmons on Smooth and Tough Surfaces and on Gratings* (Springer, Berlin, 1988)
2. A. Kocabas, A. Dana, A. Aydinli, Appl. Phys. Lett. **89**, 041123 (2006)
3. K.F. MacDonald, Z.L. Samson, M.I. Stockman, N.I. Zheludev, Nat. Photonics **3**, 55 (2009)
4. F. Yu, S.J. Tian, D.F. Yao, W. Knoll, Anal. Chem. **76**, 3530 (2004)
5. S.J. Tian, N.R. Armstrong, W. Knoll, Langmuir **21**, 4656 (2005)
6. A.W. Wark, H.J. Lee, A.J. Qavi, R.M. Corn, Anal. Chem. **79**, 6697 (2007)
7. B.K. Singh, A.C. Hillier, Anal. Chem. **80**, 3803 (2008)
8. W.-H. Yeh, J. Kleingartner, A.C. Hillier, Anal. Chem. **82**, 4988 (2010)
9. Y.J. Liu, Y.B. Zheng, J. Liou, I.-K. Chiang, I.C. Khoo, T.J. Huang, J. Phys. Chem. C **115**, 7717 (2011)
10. Y.J. Liu, X.W. Sun, P. Shum, H.P. Li, J. Mi, W. Ji, X.H. Zhang, Appl. Phys. Lett. **88**, 061107 (2006)
11. E.S.P. Leong, Y.J. Liu, B. Wang, J.H. Teng, ACS Appl. Mater. Interfaces **3**, 1148 (2011)
12. T.W. Ebbesen, H.J. Lezec, H.F. Ghaemi, T. Thio, P.A. Wolff, Nature **391**, 667 (1998)
13. Y.J. Liu, E.S.P. Leong, B. Wang, J.H. Teng, Plasmonics **6**, 659 (2011)
14. S.X. Xie, H.J. Li, S.L. Fu, H.Q. Xu, X. Zhou, Z.M. Liu, Opt. Commun. **283**, 4017 (2010)